

Floquet control of the gain and loss in a \mathcal{PT} -symmetric optical coupler

Yi Wu¹, Bo Zhu², Shu-Fang Hu³, Zheng Zhou^{4,*}, Hong-Hua Zhong^{3,†}

¹Department of Physics, Engineering University of CAPF, Xi'an 710086, China

²School of Physics and Astronomy, Sun Yat-Sen University (Zhuhai Campus), Zhuhai 519082, China

³Institute of Mathematics and Physics, Central South University of Forestry and Technology, Changsha 410004, China

⁴Department of Physics, Hunan Institute of Technology, Hengyang 421002, China

Corresponding authors. E-mail: *zhouzheng872@163.com, †hhzhong115@163.com

Received June 13, 2016; accepted November 4, 2016

Controlling the balanced gain and loss in a \mathcal{PT} -symmetric system is a rather challenging task. Utilizing Floquet theory, we explore the constructive role of periodic modulation in controlling the gain and loss of a \mathcal{PT} -symmetric optical coupler. It is found that the gain and loss of the system can be manipulated by applying a periodic modulation. Further, such an original non-Hermitian system can even be modulated into an effective Hermitian system derived by the high-frequency Floquet method. Therefore, compared with other \mathcal{PT} symmetry control schemes, our protocol can modulate the unbroken \mathcal{PT} -symmetric range to a wider parameter region. Our results provide a promising approach for controlling the gain and loss of a realistic system.

Keywords \mathcal{PT} symmetry, periodic modulation, optical coupler

PACS numbers 11.30.Er, 42.81.Qb, 42.82.Et

1 Introduction

Parity-time (\mathcal{PT}) symmetry, which is the invariance under simultaneous parity and time reversal transformation, plays an important role in non-Hermitian (NH) quantum mechanics and optics [1–3], with potential applications in optical beam engineering, mode conversion, image processing, laser mode selection, asymmetric transmission, and other fields [4–18]. The \mathcal{PT} symmetry of a Hamiltonian is defined as $\mathcal{P}TH = H\mathcal{P}T$ with the parity operator ($\hat{P} : \hat{x} \rightarrow -\hat{x}, \hat{p} \rightarrow -\hat{p}$) and time-reversal operator ($\hat{T} : \hat{x} \rightarrow \hat{x}, \hat{p} \rightarrow -\hat{p}, i \rightarrow -i, t \rightarrow -t$), where \hat{x} is the position operator, \hat{p} is the momentum operator, and t denotes time. As the operators \mathcal{PT} and H may share common eigenfunctions, a broad class of non-Hermitian \mathcal{PT} -symmetric Hamiltonians can still have entirely real eigenvalue spectra. However, depending on the values of the gain and loss parameters, the \mathcal{PT} -symmetry may be spontaneously broken [19, 20], and then the eigenvalues become complex. In the last few years, \mathcal{PT} -symmetry and \mathcal{PT} -symmetry-breaking have been observed in sev-

eral optical experiments [21–24].

An important issue in a \mathcal{PT} -symmetric system is the ability to control and tune the \mathcal{PT} phase transition. One possibility is obviously to vary the level of gain and loss in the system; however, this is a rather challenging task, as the gain and loss should remain balanced and thus must be tuned simultaneously. In recent years, it has been proposed that periodic modulations can be used to control \mathcal{PT} -symmetry in two-state systems [25–30]. It has been found that pseudo- \mathcal{PT} -symmetry may appear whether or not the original system is \mathcal{PT} -symmetric, and spontaneous \mathcal{PT} -symmetry-breaking sensitively depends on the modulation parameters [26]. These methods are based on the high-frequency Floquet method to rescale the coupling strength. Therefore, the unbroken \mathcal{PT} -symmetric range only can be modulated narrow. Another means of control is to geometrically twist the fiber [31], which can introduce additional Peierls phases in the coupling constants among the fiber, and thus the transition from unbroken to broken \mathcal{PT} -symmetric phases can be conveniently controlled. Although there are several studies on the manipulation of \mathcal{PT} -symmetry, how to control the balanced gain and loss is still lacking.

In this paper, we investigate how to control the bal-

*arXiv: 1612.04628.

anced gain and loss in a \mathcal{PT} -symmetric optical coupler by periodically modulating the coupling strength between two waveguides. Using the high-frequency Floquet method, the modulated system is effectively described by an effective averaged system whose gain and loss can be modulated by adjusting the modulation amplitude or frequency. Such an original non-Hermitian system can even be modulated into an effective Hermitian system. The spontaneous \mathcal{PT} -symmetry-breaking transition is analytically derived and is well consistent with the numerical simulation. It is revealed that the unbroken \mathcal{PT} -symmetric range can be modulated to a wider parameter region.

The structure of this article is as follows. In Section 2, we explore the constructive role of periodic modulation in controlling the gain and loss of a \mathcal{PT} -symmetric optical coupler. In Section 3, we study the Floquet modulation of \mathcal{PT} -symmetry and the corresponding dynamics. In Section 4, the possibility of experimentally observing our theoretical predictions is discussed. In the last section, we briefly summarize our results.

2 Control of the gain and loss

We consider a periodically modulated linear \mathcal{PT} -symmetric coupler that is described by the following coupled-mode equation:

$$\begin{aligned} i \frac{dc_1}{dz} &= \left[\frac{v}{2} + \frac{F \cos(\omega z)}{2} \right] c_2 + i\gamma c_1, \\ i \frac{dc_2}{dz} &= \left[\frac{v}{2} + \frac{F \cos(\omega z)}{2} \right] c_1 - i\gamma c_2. \end{aligned} \quad (1)$$

Here, $c_1(z)$ and $c_2(z)$ are the complex amplitudes and z is the coordinate in the propagation direction. Parameter v is the interchannel coupling strength, γ is the gain or loss strength, F is the modulation amplitude, and ω is the modulation frequency. Obviously, by defining the parity operator as \hat{P} , which interchanges the two channels labeled by 1 and 2, and the time-reversal operator as \hat{T} : $i \rightarrow -i$, $z \rightarrow -z$, which reverses the propagation direction, the Hamiltonian \hat{H} of system (1) is \mathcal{PT} symmetric because $\hat{P}\hat{T}\hat{H}\hat{P}\hat{T} = \hat{H}$. To simplify, below we only consider the case of $v > 0$, as the system is invariant under the transformation $c_2 \rightarrow -c_2$, $v \rightarrow -v$ and all the parameters are dimensionless throughout this paper.

By making use of the linear combinations $\psi_1 = c_1 - c_2$ and $\psi_2 = c_1 + c_2$, we can rewrite Eq. (1) as

$$i \frac{d}{dz} \begin{pmatrix} \psi_1 \\ \psi_2 \end{pmatrix} = \begin{pmatrix} -\frac{v + F \cos(\omega z)}{2} & i\gamma \\ i\gamma & \frac{v + F \cos(\omega z)}{2} \end{pmatrix} \begin{pmatrix} \psi_1 \\ \psi_2 \end{pmatrix}. \quad (2)$$

Under the condition $\gamma \ll \max[\omega, \sqrt{|F|\omega}]$, one can perform high-frequency Floquet analysis. Then, by introducing the transformation

$$\begin{aligned} \psi_1 &= \psi'_1 \exp \left[i \frac{F}{2\omega} \sin(\omega z) \right], \\ \psi_2 &= \psi'_2 \exp \left[-i \frac{F}{2\omega} \sin(\omega z) \right] \end{aligned} \quad (3)$$

and averaging the high-frequency terms, one can obtain the effectively unmodulated system

$$i \frac{d}{dz} \begin{pmatrix} \psi'_1 \\ \psi'_2 \end{pmatrix} = \begin{pmatrix} -\frac{v}{2} & i\gamma_{eff} \\ i\gamma_{eff}^* & \frac{v}{2} \end{pmatrix} \begin{pmatrix} \psi'_1 \\ \psi'_2 \end{pmatrix} \quad (4)$$

with the rescaled gain and loss parameter

$$\gamma_{eff} = \gamma \sum_{k=-\infty}^{\infty} (ie^{i\omega t})^k J_k(F/\omega). \quad (5)$$

Here, $J_k(F/\omega)$ are ordinary Bessel functions. Therefore, the modulus of γ_{eff} depends on the values of F/ω , and can change from γ to zero at some specific values of F/ω (such as $F/\omega \simeq 2.4$ and 5.52), as shown in Fig. 1. When $|\gamma_{eff}| = 0$, the effective system corresponds to a Hermitian system. Surprisingly, in contrast to our conventional understanding, we find that the gain and loss of system can be manipulated by applying a periodic modulation, and even an original non-Hermitian system can be modulated into an effective Hermitian system. As is well known, the change of the gain and loss parameter is connected to the transition from unbroken to broken \mathcal{PT} symmetry. Our results imply that the unbroken \mathcal{PT} -symmetric range can be modulated wide, which is different from previous results [26–29], where the unbroken \mathcal{PT} -symmetric range only can be modulated narrow.

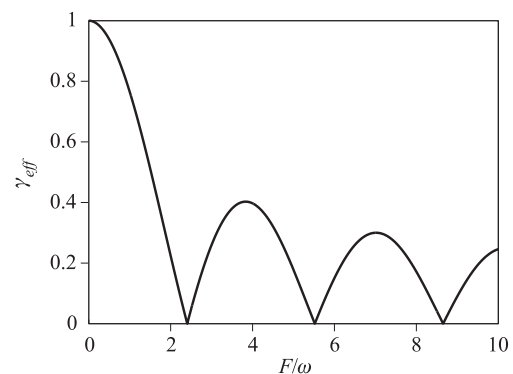


Fig. 1 Parametric dependence of the effective gain and loss $|\gamma_{eff}|$ for $\gamma = 1$ and $\omega = 10$.

3 Manipulation of \mathcal{PT} symmetry and dynamics

By diagonalizing the Hamiltonian for effective model (4), two eigenvalues can be easily determined by

$$\varepsilon = \pm |\gamma_{eff}| \sqrt{\left(\frac{v}{2|\gamma_{eff}|}\right)^2 - 1}. \quad (6)$$

Obviously, dependent on the values of $v/2|\gamma_{eff}|$, the two eigenvalues can be real or complex. The two eigenvalues are real if $v > 2|\gamma_{eff}|$, and they become complex if $v < 2|\gamma_{eff}|$. Therefore, $v = 2|\gamma_{eff}|$ is the critical point for the phase transition between the real and complex spectra in the effective system, which corresponds to original system (2) under high-frequency modulation. The spontaneous \mathcal{PT} -symmetry-breaking transition takes place in effective model (4) when the imaginary part $|\text{Im}(\varepsilon)|$ changes from zero to nonzero. Note that because $|\gamma_{eff}|$ can be modulated from γ to 0, the unbroken \mathcal{PT} -symmetric range can be modulated wide by tuning the amplitude of periodic modulation for a fixed v .

To show the parametric dependence of $|\text{Im}(\varepsilon)|$, in Figs. 2(a) and (b), we show $|\text{Im}(\varepsilon)|$ as a function of F/ω and γ for both a small coupling strength $v = 0.1$ and large coupling strength $v = 1$ with $\omega = 10$. First, it is clear that, compared with a \mathcal{PT} -symmetric system with no modulation, the region of \mathcal{PT} symmetry in our modulated system can obviously be manipulated to be wider by tuning F/ω , which is different to previous results [26, 28, 29]. Second, near a minimum of $|\gamma_{eff}|$ such as $F/\omega \simeq 2.4$, despite the size of v and γ , there always exists a completely real quasienergy spectrum.

According to the Floquet theorem, one can use a nu-

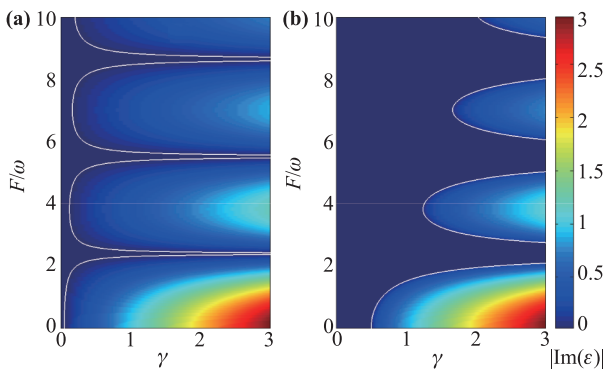


Fig. 2 The imaginary parts of the quasienergies $|\text{Im}(\varepsilon)|$ as a function of F/ω and γ for different coupling strengths $v = 0.1$ (a) and $v = 1$ (b). The other parameter is fixed as $\omega = 10$. The white curves are the boundary ($\gamma_{eff} = v/2$) between $|\text{Im}(\varepsilon)| = 0$ and $|\text{Im}(\varepsilon)| \neq 0$.

merical method to calculate the Floquet states and their quasienergies for arbitrary modulation amplitude and frequency. The Floquet states of modulated system (1) satisfy $c_j(z) = e^{-i\varepsilon z} \tilde{c}_j(z)$ for $j = 1, 2$, where propagation constant ε is designated as the quasienergy, and complex amplitudes $\tilde{c}_j(z)$ are periodic with modulation period $T = 2\pi/\omega$. The quasienergies and amplitudes of modulated system (1) are then given by

$$\mathcal{F}\tilde{c}_j(z) = \varepsilon\tilde{c}_j(z), \quad j = 1, 2, \quad (7)$$

with the Floquet operator

$$\mathcal{F} = -i\frac{d}{dz} + H(z). \quad (8)$$

To verify the validity of the above high-frequency Floquet analysis, we compare the numerical quasienergies obtained from original model (1) and analytical formula (6) obtained from effective model (4). As an example, we show the real parts $\text{Re}(\varepsilon)$ and imaginary parts $\text{Im}(\varepsilon)$ of quasienergies ε as a function of γ for different driving amplitudes $F = 5, 15$, and 24 in Fig. 3. The other parameters are chosen as $v = 0.1$ and $\omega = 10$. Obviously, in the high-frequency regime $\gamma \ll \max[\omega, \sqrt{|F|\omega}]$ the analytical (solid lines) and numerical (circles) values for the quasienergies ε are in good agreement. This clearly shows that below the critical point ($|\gamma_{eff}| < v/2$), both the numerical and analytical results confirm the entirely real quasienergy spectrum, and the transition from a completely real quasienergy spectrum ($|\text{Im}(\varepsilon)| = 0$) to a complex spectrum ($|\text{Im}(\varepsilon)| \neq 0$) can take place when γ increases. In particular, in contrast to a \mathcal{PT} -symmetric system without periodic modulation, the spontaneous \mathcal{PT} -symmetry-breaking transition can be manipulated by tuning the modulation parameter. For small F , for example $F = 5$ in Fig. 3(b), one clearly sees that there exists a narrow real quasienergy spectrum region, and the spontaneous \mathcal{PT} -symmetry-breaking transition takes place at $\gamma \doteq 0.05$. For a bigger F , such as $F = 15$, the region of the real quasienergy spectrum broadens and the spontaneous \mathcal{PT} -symmetry-breaking transition occurs at $\gamma_c \doteq 0.1$ [see Fig. 3(d)]. The quasienergy spectrum is always completely real regardless of the size of γ for $F = 24$, which is equivalent to a Hermitian case, as shown in Fig. 3(f).

To understand this concept from another angle, we also show the quasienergy dependence on modulation parameter F/ω for different parameters v in Fig. 4. The other parameters are chosen as $\gamma = 1$ and $\omega = 10$. As shown in Figs. 4(a) and (b), for a small coupling strength $v = 0.1$, the \mathcal{PT} symmetry can spontaneously break when parameter F/ω changes. If the coupling strength is increased to $v = 1$, a completely real quasienergy spectrum always appears when modulation parameter F/ω exceeds a critical value. These results show that the region of \mathcal{PT} symmetry can be manipulated wider by

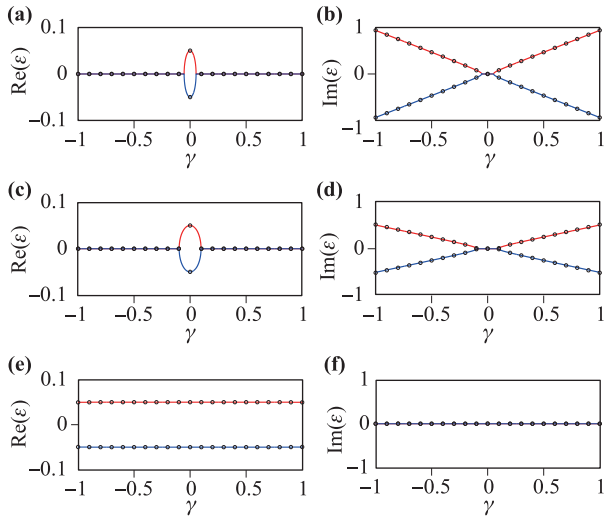


Fig. 3 The real parts $\text{Re}(\varepsilon)$ and the imaginary parts $\text{Im}(\varepsilon)$ of the complex quasienergies as a function of γ for different driving amplitudes $F = 5$ (top row), $F = 15$ (middle row) and $F = 24$ (bottom row). The solid lines correspond to analytical results given by the formula (6) for the effective model (4) and the circles correspond to numerical results obtained from the original model (1). The other parameters are $v = 0.1$ and $\omega = 10$.

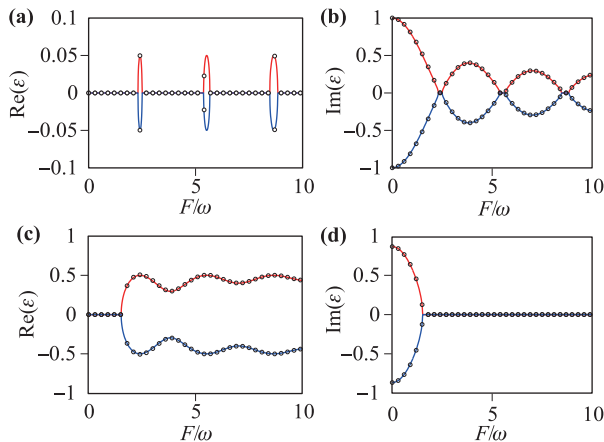


Fig. 4 The real parts $\text{Re}(\varepsilon)$ and the imaginary parts $\text{Im}(\varepsilon)$ of the complex quasienergies as a function of F/ω for two different coupling strengths $v = 0.1$ (top row) and $v = 1$ (bottom row). The solid lines correspond to analytical results given by the formula (6) for the effective model (4) and the circles correspond to numerical results obtained from the original model (1). The other parameters are chosen as $\gamma = 1$ and $\omega = 10$.

tuning F/ω in the case of bigger coupling strength for a fixed parameter γ .

In the following, through numerical integration, we analyze the light propagation in unbroken and broken \mathcal{PT} -symmetric parameter regions. To do this, we define the two intensities in coupled-mode system (1) as

$I_1(z) = |c_1(z)|^2$ and $I_2(z) = |c_2(z)|^2$, the total intensity as $I_t(z) = I_1(z) + I_2(z)$, and the time-averaged total intensity as $I_t^{av}(z) = \frac{1}{T_s} \int_z^{z+T_s} I_t(\tilde{z}) d\tilde{z}$ with $T_s = 2\pi/|\text{Re}(\varepsilon_2) - \text{Re}(\varepsilon_1)|$ being the two real parts of ε . In Fig. 5, for $v = 1$, $\gamma = 1$, and $\omega = 10$, we show the evolution in intensity from initial states $c_1(0) = 1$ and $c_2(0) = 0$ for $F/\omega = 1.52$ [broken \mathcal{PT} -symmetric parameter, see Fig. 2(b)] and $F/\omega = 2.0$ [unbroken \mathcal{PT} -symmetric parameter, see Fig. 2(b)]. We can see that the light propagation sensitively depends upon the \mathcal{PT} symmetry. Stationary light propagations of bounded intensity oscillations appear if the \mathcal{PT} symmetry of the Hamiltonian is unbroken, where all quasienergies are real [see Fig. 5(b)]. Nonstationary light propagations of unbounded intensity oscillations appear if the \mathcal{PT} symmetry of the Hamiltonian is broken, where at least one of the quasienergies is complex [see Fig. 5(a)]. Therefore, the propagation dynamics of our modulated system (1) also can be manipulated by tuning the modulation parameter.

4 Optical realization

Below, we discuss the experimental possibility of observing our theoretical predictions. Recently, several \mathcal{PT} -symmetric optical systems were experimentally realized [21, 22, 32–34]. The complex refractive index of gain or loss effects can be obtained from quantum-well lasers or photorefractive structures through two-wave mixing [35, 36]. Further, periodic modulations can be introduced by out-of-phase harmonic modulations of the real refractive index [37–40] or periodic curvature along the

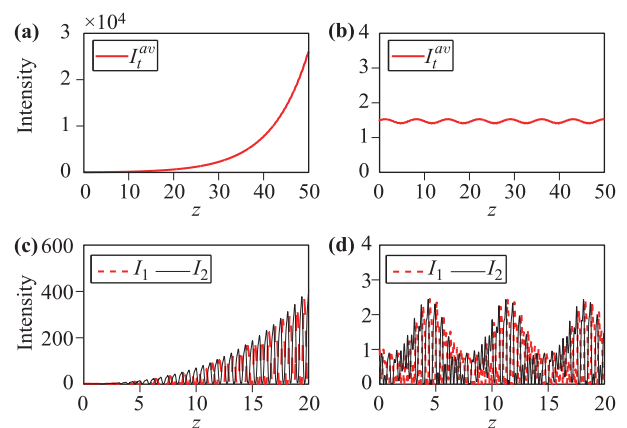


Fig. 5 Intensity evolution from Eq. (1) for the initial state of $c_1(0) = 1$ and $c_2(0) = 0$. Upper row: long-distance time averaged total intensity evolution for (a) $F/\omega = 1.52$ and (b) $F/\omega = 2.0$. Lower row: short-distance intensity evolution for (c) $F/\omega = 1.52$ and (d) $F/\omega = 2.0$. The other parameters are chosen as $v = 1$, $\gamma = 1$ and $\omega = 10$.

propagation direction [37, 38, 41, 42]. In our system, the propagation of a light wave along the z axis obeys the wave equation for its dimensionless electric field amplitude $\phi(x, z)$:

$$i \frac{\partial \phi(x, z)}{\partial z} = -\frac{1}{2k} \frac{\partial^2 \phi(x, z)}{\partial x^2} + V(x, z)\phi(x, z) \quad (9)$$

with refractive index $V(x, z) = V_R(x, z) + iV_I(x)$. The real part is $V_R(x, z) = V_0(x) + V_1(x, z)$ with the symmetric double-well function $V_0(x)$ and periodic modulation $V_1(x, z)$, which periodically changes the distance between two waveguides. The imaginary part $V_I(-x) = -V_I(x)$ consists of antisymmetric functions, and in order to guarantee the \mathcal{PT} -symmetry of our system, we defined $f(z)$ to be a periodic even function. In our numerical simulations, we chose

$$\begin{aligned} V_0(x) &= -\rho \left(\exp \left[-\left(\frac{x + \frac{\omega_s}{2}}{\omega_x} \right)^6 \right] \right. \\ &\quad \left. + \exp \left[-\left(\frac{x - \frac{\omega_s}{2}}{\omega_x} \right)^6 \right] \right), \\ V_1(x, z) &= -\rho\alpha \left(\exp \left[-\left(\frac{x + \frac{f(z)}{2}}{\omega_x} \right)^6 \right] \right. \\ &\quad \left. + \exp \left[-\left(\frac{x - \frac{f(z)}{2}}{\omega_x} \right)^6 \right] \right), \\ V_I(x) &= -\rho\beta \left(\exp \left[-\left(\frac{x + \frac{\omega_s}{2}}{\omega_x} \right)^6 \right] \right. \\ &\quad \left. - \exp \left[-\left(\frac{x - \frac{\omega_s}{2}}{\omega_x} \right)^6 \right] \right), \\ f(z) &= \omega_s - \mu A \cos(\omega z). \end{aligned} \quad (10)$$

Here, $(\rho, \alpha, \beta, \mu)$ are four parameters describing the refractive index, and ω_x is the waveguide width. Further, $f(z)$ denotes the modulation of the refractive index where ω_s is the distance between two waveguides. Parameters A and ω are the modulation amplitude and frequency, respectively. Parity operator $\hat{P} : \hat{x} \rightarrow -\hat{x}$ and $\hat{p} \rightarrow -\hat{p}$ has the effect of reversing the transverse direction. Time-reversal operator $\hat{T} : \hat{x} \rightarrow \hat{x}, \hat{p} \rightarrow -\hat{p}, i \rightarrow -i$ and $z \rightarrow -z$, has the effect of reversing the propagation direction. Therefore, the waveguide would be \mathcal{PT} -symmetric if $V(x, z) = V^*(-x, -z)$, where the asterisk “*” represents complex conjugation.

To demonstrate how to control \mathcal{PT} symmetry by periodically modulating the distance between two waveguides, we simulated the two-channel coupler by directly integrating the continuous wave equation (9). In our numerical simulation, the initial states were chosen to be the lowest Wannier modes for isolated individual waveguides, and parameter k was set to $k = 1$. Fixing $\omega_s = 3.2$,

$\omega_x = 0.3$, $\mu = 0.4$, $\rho = 2.78$, $\alpha = 1$, $\beta = 0.0252$, and $\omega = 0.22$, we simulated continuous wave equation (9) for different modulation amplitudes A . As in Refs. [39, 40], ω_x and ω_s are in units of $10 \mu\text{m}$, and $\rho = 2.78$ corresponds to a real refractive index of 3.1×10^{-4} .

According to the analytical analysis in Section 3, if the \mathcal{PT} symmetry of the Hamiltonian is unbroken, the light propagations are stationary oscillations, and nonstationary light propagations of the unbounded intensity oscillations appear if the \mathcal{PT} symmetry of the Hamiltonian is broken. As an analogy, we numerically explore the light propagation in a \mathcal{PT} -symmetric coupler under different modulation amplitudes. In Fig. 6, the left column shows the refractive index distributions $V(x, z)$ and the right column shows the light propagation $|\phi(x, z)|^2$ obtained by numerically integrating continuous wave equation (9). First, for comparison, in Figs. 6(a) and (b) we use the unmodulated system in the region of broken \mathcal{PT} symmetry as a reference system. Light propagation $|\phi(x, z)|^2$ shows nonstationary oscillations with a growing total intensity for this unmodulated waveguide [see Fig. 6(b)]. In contrast to the unmodulated case $A/\omega = 0$, the stationary periodic oscillations of light propagation $|\phi(x, z)|^2$ confirm the existence of \mathcal{PT} symmetry in the modulated cases $A/\omega = 1.5$ and $A/\omega = 2.4$ [Figs. 6(d) and (f)]. Specifically, when the modulated parameter approaches the zero point of the Bessel function, light propagation $|\phi(x, z)|^2$ demonstrates more periodic oscillations with propagation behavior that is similar to that of a modulated Hermitian coupler. This means that the unbroken \mathcal{PT} -symmetric range can be modulated to span a wider parameter region by periodically modulating the

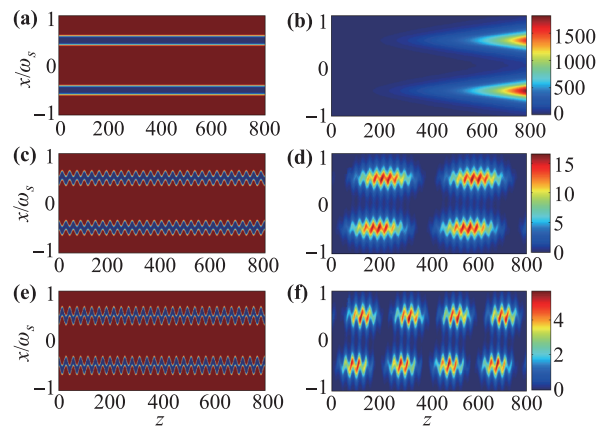


Fig. 6 Light propagation in a \mathcal{PT} -symmetric two-channel coupler. First row: (a) the refractive index distribution $V(x, z)$ and (b) the light propagation $|\phi(x, z)|^2$ for unmodulated waveguides. Second row: (c) the refractive index distribution $V(x, z)$ and (d) the light propagation $|\phi(x, z)|^2$ for modulated waveguides with $A/\omega = 1.5$. Third row: (e) the refractive index distribution $V(x, z)$ and (f) the light propagation $|\phi(x, z)|^2$ for modulated waveguides with $A/\omega = 2.4$.

coupling strength of the \mathcal{PT} -symmetric optical coupler. Therefore, our simulated results are qualitatively consistent with those predicted by coupled-mode equation (1).

5 Summary

In summary, we have investigated how to control the balanced gain and loss in a \mathcal{PT} -symmetric optical coupler by periodically modulating the coupling strength between two waveguides. Using the high-frequency Floquet method, the modulated system is effectively described by an effective averaged system whose gain and loss can be modulated by adjusting the modulation amplitude or frequency, and such an original non-Hermitian system can even be modulated into an effective Hermitian system. The spontaneous \mathcal{PT} -symmetry-breaking transition was analytically derived and is quite consistent with the numerical simulation. It is revealed that the unbroken \mathcal{PT} -symmetric range can be modulated to span a wider parameter region. Furthermore, we discuss the experimental possibility of observing these theoretical results. The simulated results obtained by directly integrating the continuous wave equation are qualitatively consistent with the ones predicted by the coupled-mode equation. Our results may provide a promising approach for controlling the gain and loss of a realistic system.

Acknowledgements We acknowledge helpful discussion with Chaohong Lee. This work was supported by the National Natural Science Foundation of China (Grant Nos. 11465008, 11574405, and 11426223), the Hunan Provincial Natural Science Foundation (Grant Nos. 2015JJ2114, 2015JJ4020, and 14JJ3114), and the Scientific Research Fund of Hunan Provincial Education Department (Grant No. 14A118).

References

1. S. V. Suchkov, A. A. Sukhorukov, J. Huang, S. V. Dmitriev, C. Lee, and Y. S. Kivshar, Nonlinear switching and solitons in \mathcal{PT} -symmetric photonic systems, *Laser Photonics Rev.* 10(2), 177 (2016)
2. V. V. Konotop, J. Yang, and D. A. Zezyulin, Nonlinear waves in \mathcal{PT} -symmetric systems, *Rev. Mod. Phys.* 88(3), 035002 (2016)
3. N. Moiseyev, *Non-Hermitian Quantum Mechanics*, Cambridge: Cambridge University Press, 2011
4. H. Hodaei, M. A. Miri, M. Heinrich, D. N. Christodoulides, and M. Khajavikhan, Parity-time symmetric microring lasers, *Science* 346(6212), 975 (2014)
5. L. Feng, Z. J. Wong, R. M. Ma, Y. Wang, and X. Zhang, Single-mode laser by parity-time symmetry breaking, *Science* 346(6212), 972 (2014)
6. L. Feng, Y. L. Xu, W. S. Fegadolli, M. H. Lu, J. E. B. Oliveira, V. R. Almeida, Y. F. Chen, and A. Scherer, Experimental demonstration of a unidirectional reflectionless parity-time metamaterial at optical frequencies, *Nat. Mater.* 12(2), 108 (2012)
7. B. Peng, S. K. Ozdemir, F. Lei, F. Monifi, M. Gianfreda, G. L. Long, S. Fan, F. Nori, C. M. Bender, and L. Yang, Parity-time-symmetric whispering-gallery microcavities, *Nat. Phys.* 10(5), 394 (2014)
8. F. Nazari, N. Bender, H. Ramezani, M. K. Moravvej-Farshi, D. N. Christodoulides, and T. Kottos, Optical isolation via \mathcal{PT} -symmetric nonlinear Fano resonances, *Opt. Express* 22(8), 9574 (2014)
9. H. Xiong, L. Si, X. Yang, and Y. Wu, Asymmetric optical transmission in an optomechanical array, *Appl. Phys. Lett.* 107(9), 091116 (2015)
10. S. Longhi and L. Feng, \mathcal{PT} -symmetric microring laser absorber, *Opt. Lett.* 39(17), 5026 (2014)
11. V. A. Vysloukh and Y. V. Kartashov, Resonant mode conversion in the waveguides with unbroken and broken \mathcal{PT} symmetry, *Opt. Lett.* 39(20), 5933 (2014)
12. J. Gan, H. Xiong, L. Si, X. Lü, and Y. Wu, Soliton in optomechanical arrays, *Opt. Lett.* 41(12), 2676 (2016)
13. H. Hodaei, M. A. Miri, A. U. Hassan, W. E. Hayenga, M. Heinrich, D. N. Christodoulides, and M. Khajavikhan, Parity-time-symmetric coupled microring lasers operating around an exceptional point, *Opt. Lett.* 40(21), 4955 (2015)
14. X. Lü, H. Jing, J. Ma, and Y. Wu, \mathcal{PT} -symmetry-breaking chaos in optomechanics, *Phys. Rev. Lett.* 114(25), 253601 (2015)
15. H. Jing, S. K. Ozdemir, X. Lü, J. Zhang, L. Yang, and F. Nori, \mathcal{PT} -symmetric phonon laser, *Phys. Rev. Lett.* 113(5), 053604 (2014)
16. Y. V. Kartashov, V. A. Vysloukh, V. V. Konotop, and L. Torner, Diffraction control in \mathcal{PT} -symmetric photonic lattices: From beam rectification to dynamic localization, *Phys. Rev. A* 93(1), 013841 (2016)
17. J. Li, J. Li, Q. Xiao, and Y. Wu, Giant enhancement of optical high-order sideband generation and their control in a dimer of two cavities with gain and loss, *Phys. Rev. A* 93(6), 063814 (2016)
18. H. Wang, Multi-peak solitons in \mathcal{PT} -symmetric Bessel optical lattices with defects, *Front. Phys.* 11(5), 114204 (2016)
19. C. M. Bender and S. Boettcher, Real spectra in Non-Hermitian Hamiltonians having \mathcal{PT} symmetry, *Phys. Rev. Lett.* 80(24), 5243 (1998)
20. C. M. Bender, Making Sense of non-Hermitian Hamiltonians, *Rep. Prog. Phys.* 70(6), 947 (2007)
21. C. E. Rüter, K. G. Makris, R. El-Ganainy, D. N. Christodoulides, M. Segev, and D. Kip, Observation of parity-time symmetry in optics, *Nat. Phys.* 6(3), 192 (2010)

22. A. Guo, G. J. Salamo, D. Duchesne, R. Morandotti, M. Volatier-Ravat, V. Aimez, G. A. Siviloglou, and D. N. Christodoulides, Observation of PT-symmetry breaking in complex optical potentials, *Phys. Rev. Lett.* 103(9), 093902 (2009)
23. A. Regensburger, C. Bersch, M. A. Miri, G. Onishchukov, D. N. Christodoulides, and U. Peschel, Parity-time synthetic photonic lattices, *Nature* 488(7410), 167 (2012)
24. S. Bittner, B. Dietz, U. Günther, H. L. Harney, M. Miski-Oglu, A. Richter, and F. Schäfer, PT symmetry and spontaneous symmetry breaking in a microwave billiard, *Phys. Rev. Lett.* 108(2), 024101 (2012)
25. N. Moiseyev, Crossing rule for a PT-symmetric two-level time-periodic system, *Phys. Rev. A* 83(5), 052125 (2011)
26. X. Luo, J. Huang, H. Zhong, X. Qin, Q. Xie, Y. S. Kivshar, and C. Lee, Pseudo-parity-time symmetry in optical systems, *Phys. Rev. Lett.* 110(24), 243902 (2013)
27. X. Lian, H. Zhong, Q. Xie, X. Zhou, Y. Wu, and W. Liao, PT-symmetry-breaking induced suppression of tunneling in a driven non-Hermitian two-level system, *Eur. Phys. J. D* 68(7), 189 (2014)
28. 10.1103/PhysRevA.90.040101 Y. N. Joglekar, R. Marathe, P. Durganandini, and R. K. Pathak, PT spectroscopy of the Rabi problem, *Phys. Rev. A* 90(4), 040101(R) (2014)
29. J. Gong and Q. H. Wang, Stabilizing non-Hermitian systems by periodic driving, *Phys. Rev. A* 91(4), 042135 (2015)
30. Z. Zhou, B. Zhu, and L. Zhang, Analytical study on propagation dynamics of optical beam in parity-time symmetric optical couplers, *Commun. Theor. Phys.* 63(4), 406 (2015)
31. S. Longhi, PT phase control in circular multi-core fibers, *Opt. Lett.* 41(9), 1897 (2016)
32. R. El-Ganainy, K. G. Makris, D. N. Christodoulides, and Z. H. Musslimani, Theory of coupled optical PT symmetric structures, *Opt. Lett.* 32(17), 2632 (2007)
33. K. G. Makris, R. El-Ganainy, D. N. Christodoulides, and Z. H. Musslimani, Beam dynamics in PT symmetric optical lattices, *Phys. Rev. Lett.* 100(10), 103904 (2008)
34. Z. H. Musslimani, K. G. Makris, R. El-Ganainy, and D. N. Christodoulides, Optical solitons in PT periodic potentials, *Phys. Rev. Lett.* 100(3), 030402 (2008)
35. A. Yariv, *Optical Electronics in Modern Communications*, Oxford: Oxford University Press, 1997
36. P. Yeh, *Introduction to Photorefractive Nonlinear Optics*, Wiley Series in Pure and Applied Optics, New York: Wiley, 2001
37. S. Longhi, Quantum-optical analogies using photonic structures, *Laser Photonics Rev.* 3(3), 243 (2009)
38. I. L. Garanovich, S. Longhi, A. A. Sukhorukov, and Y. S. Kivshar, Light propagation and localization in modulated photonic lattices and waveguides, *Phys. Rep.* 518(1–2), 1 (2012)
39. A. Szameit, Y. V. Kartashov, F. Dreisow, M. Heinrich, T. Pertsch, S. Nolte, A. Tünnermann, V. A. Vysloukh, F. Lederer, and L. Torner, Inhibition of light tunneling in waveguide arrays, *Phys. Rev. Lett.* 102(15), 153901 (2009)
40. A. Szameit, Y. V. Kartashov, M. Heinrich, F. Dreisow, R. Keil, S. Nolte, A. Tünnermann, V. A. Vysloukh, F. Lederer, and L. Torner, Nonlinearity-induced broadening of resonances in dynamically modulated couplers, *Opt. Lett.* 34(18), 2700 (2009)
41. G. Della Valle, M. Ornigotti, E. Cianci, V. Foglietti, P. Laporta, and S. Longhi, Visualization of coherent destruction of tunneling in an optical double well system, *Phys. Rev. Lett.* 98(26), 263601 (2007)
42. J. M. Zeuner, N. K. Efremidis, R. Keil, F. Dreisow, D. N. Christodoulides, A. Tünnermann, S. Nolte, and A. Szameit, Optical analogues for massless Dirac particles and conical diffraction in one dimension, *Phys. Rev. Lett.* 109(2), 023602 (2012)